DNA Origami Templated Growth of Multilamellar Lipid Assemblies

Sofia Julin,[†] Nonappa,[‡$],Boxuan Shen[†] Veikko Linko,[†,‡] and Mauri A. Kostiainen*[†,‡]

† Biohybrid Materials, Department of Bioproducts and Biosystems, Aalto University, 00076 Aalto, Finland

[‡] HYBER Centre, Department of Applied Physics, Aalto University, 00076 Aalto, Finland

[$] Faculty of Engineering and Natural Sciences, Tampere University, FI-33720, Tampere, Finland

KEYWORDS: DNA origami, lipid multilayers, DOTAP, self-assembly, electrostatic interactions, DNase I digestion

ABSTRACT

Lipids are important building blocks in cellular compartments and their supramolecular self-assembly into well-defined hierarchical structures has gained increasing interest. DNA form highly-ordered assemblies, lipoplexes, when combined with cationic liposomes and extensive experimental work has been conducted on these lipoplexes. However, for many potential applications the variety of the structural morphology of lipoplexes is still rather limited. Here, we have complexed larger DNA origami nanostructures and the cationic lipid DOTAP and studied their self-assembly driven by electrostatic and hydrophobic interactions. The results suggest that

the DNA origami function as a template for the growth of multilamellar lipid structures and that the DNA origamis are embedded in the formed lipid matrix. Furthermore, the lipid encapsulation was found to significantly shield the DNA origami against nuclease digestion. The presented complexation strategy is suitable for a wide range of DNA-based templates and could therefore find uses in construction of cell-membrane associated components.

INTRODUCTION

Inspired by the complex biological structures found in nature, supramolecular self-assembly has emerged as an attractive approach to construct novel functional nanoscale materials with unique properties.[1] Many compartmentalized structures found in biological systems are formed by lipids, and their self-assembly has gained increasing interests during recent years.[2,3] DNA-lipid complexes (lipoplexes) are highly ordered supramolecular assemblies that are formed through electrostatic and other non-covalent interactions between the negatively charged phosphate groups in the DNA backbone and cationic liposomes.[4] Lipoplexes have potential applications in *e.g.* drug and gene delivery,[4–7] optoelectronics and synthetic chemistry,[7] and therefore extensive experimental work has been carried out to understand both the driving forces behind the lipoplex assembly and the structural morphology of the formed complexes.[8] Lipoplexes may adopt several different supramolecular arrangements, and it is known that the lipid packing parameters have a remarkable role in the structural organization of the components.[4,9] The most frequently observed lipoplex arrangement is the lamellar phase (L_α) consisting of alternating lipid bilayers and monolayers of parallel DNA molecules.[10] Another commonly occurring structure is the inverted hexagonal phase (H_{II}) in which lipid monolayer-coated DNA molecules are arranged on a hexagonal lattice.[11] In addition, both a hexagonal phase (H_I), where tubular lipid micelles arranged

on a hexagonal lattice are enclosed in a DNA lattice with honeycomb symmetry,[12] and a double gyroid cubic phase structure (Q_{II})[13] have been reported.

Thus far, the variety of the structural morphology of the lipoplexes have been rather limited, and therefore it would be desirable to study whether larger DNA nanostructures with higher structural complexity could be used similarly to form ordered assemblies. Over the past two decades, there has been a rapid development in the field of DNA nanotechnology and DNA has emerged as an effective and programmable building material for nanoscale fabrication.[14,15] In particular the DNA origami technique has enabled highly accurate production of a wide range of custom-designed DNA-based nanostructures,[16] which have paved the way for applications such as *e.g.* drug carriers,[17,18] artificial membrane channels[19–21] and templates for precise arrangements of molecular components.[22,23] Moreover, due to the phosphate groups in the DNA backbone, the DNA origami structures are highly negatively charged and therefore suitable also as building blocks in ordered assemblies held together purely *via* electrostatic interactions, which has been previously demonstrated with gold nanoparticles[24] and collagen-mimetic peptides.[25] However, for many potential applications, in particular in biomedicine, the structural stability of the DNA origami is still questionable, as the DNA origamis are for example readily degraded by nucleases, such as DNase I.[26,27] Therefore, to increase the stability of the DNA origamis under biologically relevant conditions, several coating strategies have been proposed, including viral envelope-mimicking lipid bilayers,[28] glutaraldehyde cross-linked PEGylated oligolysine[29] and electrostatically driven coatings with cationic polymers,[30–33] serum albumin-dendron conjugates[34] and -derivatives[35], virus capsid proteins[36] and chitosan.[33]

In this work, we have electrostatically assembled three different DNA origami nanostructures with a cationic lipid 1,2-dioleoly-3-trimethylammonium-propane (DOTAP) (Figure 1). Further, to gain

additional insights into the assembly process the effect of size and shape of the DNA nanostructure as well as the stoichiometric ratio between the DOTAP molecules and the DNA origamis ($n_{DOTAP}/n_{origami}$) have been investigated. The electrostatic binding between the DOTAP molecules and the DNA origami was studied using agarose gel electrophoretic mobility shift assay (EMSA) and the morphology of the formed complexes characterized using conventional transmission electron microscopy (TEM), cryogenic transmission electron microscopy (cryo-TEM), transmission electron tomography (ET) reconstruction and energy-dispersive X-ray spectroscopy (EDS). The results reveal that DNA origami could function as a nucleation site for the growth of multilamellar lipid assemblies and that the DNA origami are embedded in the formed lipid matrix. Moreover, DNase I digestion experiments show that the multilamellar lipid matrix also protect the DNA origami against enzymatic digestion, but to which extent the DNA origamis are embedded in and shielded by the lipid matrix is highly dependent on the DNA origami shape.

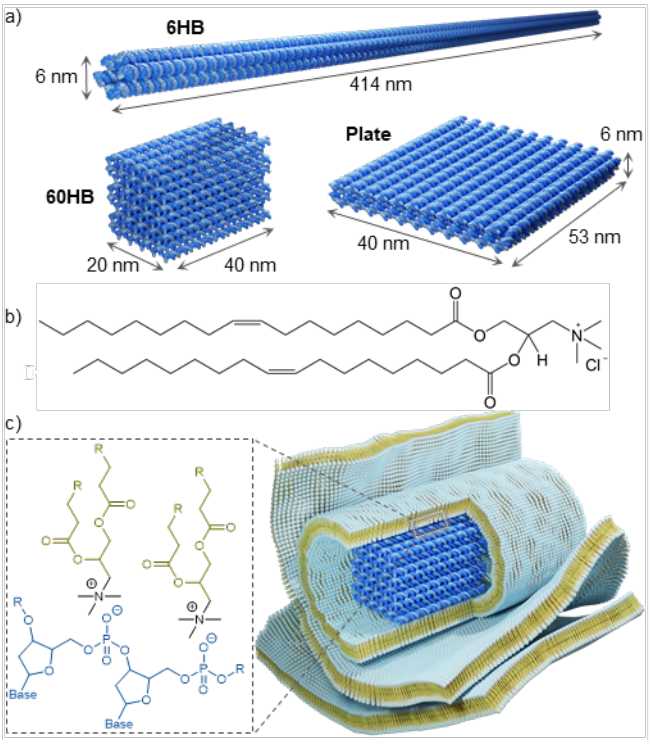

Figure 1. Building blocks used in the study and their electrostatic assembly. (a) The design and outer dimensions of the three DNA origami structures used in the study: 6-helix bundle (6HB), 60-helix bundle (60HB) and plate. (b) The chemical structure of the cationic lipid 1,2-dioleoly-3-trimethylammonium-propane (DOTAP). (c) Multilamellar lipid structures shielding the DNA origami are formed through electrostatic interactions between the positively charged head group of the DOTAP molecules and the phosphate groups in the DNA backbone.

RESULTS AND DISCUSSION

For this study, three DNA origami nanostructures with different aspect ratios; a 6-helix bundle (6HB), a 60-helix bundle (60HB) and a plate (Figure 1a), were prepared using standard annealing procedures (see the Supporting Information for preparation details and characterization data). For all experiments, the storage medium of the DNA origamis was exchanged to deionized water using the previously described spin-filtering method.[37] Further, DOTAP was chosen as the cationic lipid

since it is biodegradable and one of the most commonly employed cationic lipids for lipoplex assembly.[38] DOTAP has a quaternary ammonium head group and is hence positively charged over a wide pH range (Figure 1b). Free ions in the surrounding media effectively screen the electrostatic interactions between charged components[39] and therefore the complexation was carried out in the absence of added electrolytes. Under these conditions, the electrostatic interactions between the positively charged DOTAP head groups and the negatively charged phosphate groups in the DNA backbone were promoted, which facilitates the formation of DNA origami – lipid complexes and the growth of a multilamellar lipid matrix around the DNA origami (Figure 1c).

Initially, the electrostatic binding of DOTAP to the DNA origamis and the formation of assemblies was studied by agarose gel electrophoretic mobility shift assay (EMSA) (Figure 2, left column). When the cationic lipids bind to the negatively charged DNA origami surface, their electrophoretic mobility in the gel is altered. Therefore, the stoichiometric ratio $n_{DOTAP}/n_{origami}$ required for the assembly formation was determined by adding increasing amounts of DOTAP solution (dissolved in ethanol) to a constant amount of DNA origami solution (in deionized water, constant final concentration of 7.5 nM). For all three DNA origamis, a clear gradual decrease in the electrophoretic mobility was observed, and at a stoichiometric ratio of $n_{DOTAP}/n_{origami} \sim 5000$, the DNA origamis were completely immobilized in the gel. Further, after the gel run, the immobile DNA origami – lipid complexes, observed at high stoichiometric ratios, were also visible with the naked eye as precipitates in the gel wells.

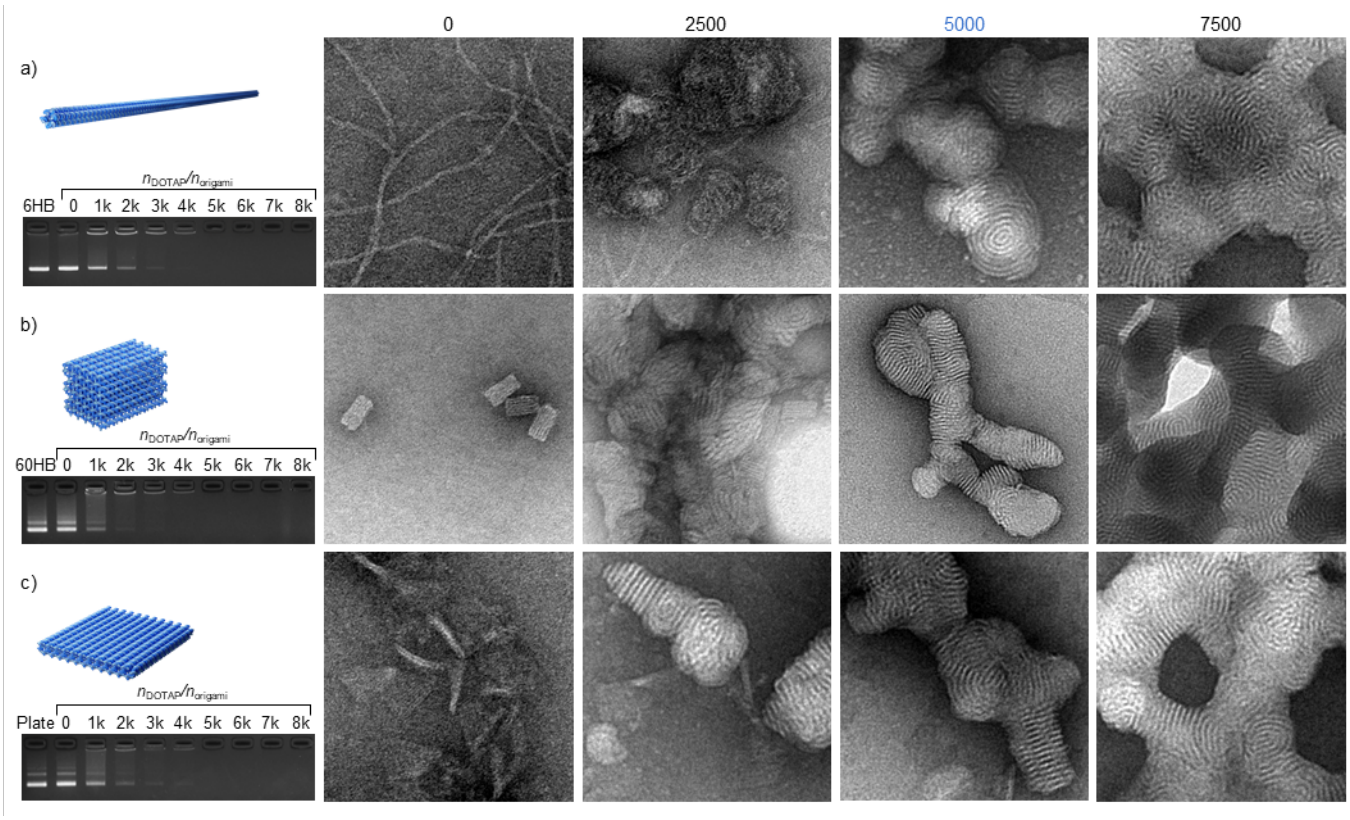

Figure 2. Electrostatic binding of positively charged DOTAP to (a) 6HB (b) 60HB and (c) plate DNA origamis and the formation of DNA origami – lipid assemblies. The left panel shows agarose gel electrophoretic mobility shift assay (EMSA) for a constant amount of DNA origami (in deionized water, constant final concentration of 7.5 nM) complexed with increasing amounts of DOTAP (dissolved in ethanol). Lane 1 (6HB, 60HB or Plate) is a control sample without any added ethanol, and the final ethanol concentration in all other samples is approximately 9 % (w/v). The right panel shows transmission electron microscopy (TEM) images of the formed complexes at different stoichiometric ratios between the DOTAP and DNA origami ($n_{DOTAP}/n_{origami}$). The samples are negatively stained with uranyl formate (2 % (w/v)) and the size of all TEM images are 250 nm × 250 nm.

To obtain information about the structural morphology of the complexes, we used TEM to characterize the assemblies formed using all three kind of DNA origamis at different stoichiometric ratios, $n_{DOTAP}/n_{origami}$. (Figure 2, right panel). Although there are morphological variations depending on the used DNA origami, similar trends were observed for all studied structures. The TEM images prepared at $n_{DOTAP}/n_{origami} = 0$ show, as expected, distinct and intact DNA origamis, which also confirms that the DNA origami structures maintain their structural stability in the aqueous ethanol solution (9 % (w/v), $c_{MgCl_2} \leq 0$ mM) used for the assembly. Further, the thin double-layer plates have low contrast and they tend to stand on their edges and get slightly twisted, which has been reported also previously for similar DNA origamis (see S3 for additional TEM images that verify the correct folding).[40] When DOTAP is added to the DNA origami solution, the cationic lipid molecules bind electrostatically to the negatively charged DNA origami surface, which most likely nucleates the formation of the observed multilamellar complexes. The samples with a relative excess of DNA origami ($n_{DOTAP}/n_{origami}$ ~2500) still contain free DNA origami, but small fingerprint-like assemblies start to appear at the interfaces of the DNA origamis. The DNA origamis are also more aggregated, indicating that the DOTAP molecules function as a supramolecular "glue" that bring the DNA origamis together. At the optimal stoichiometric ratio of $n_{DOTAP}/n_{origami}$ ~5000, mostly distinct multilamellar complexes, a few hundreds of nanometers in size, are formed without any free DNA origami to be observed. When the DOTAP concentration is further increased and the DOTAP are in excess ($n_{DOTAP}/n_{origami}$ ~7500), the TEM images reveal even larger multilamellar assemblies up to several micrometers in size. Morphologically, the formed multilamellar structures resemble lipoplexes assembled using DOTAP,[38] but also lamellarsomes formed through the self-assembly of amphiphilic block copolymers in water.[41]

The binding of the cationic DOTAP molecules to the negatively charged DNA origami surface and subsequent formation of larger multilamellar assemblies is a highly cooperative process driven by the interplay between electrostatic and hydrophobic interactions.[42] For example, in the case of the complexes formed using the 6HB, the structural features observed in the TEM images can be explained by a cooperative process that proceeds in a stepwise manner (Figure 3a). The 6HB is mechanically rather flexible, and when the cationic DOTAP molecules bind to the negatively charged origami surface, the 6HB will wrap into highly packed 'ball of yarn'-like assemblies. In order to minimize the undesired interactions between the aqueous phase and the hydrophobic lipid tails, DOTAP molecules bound to different parts of the 6HB will get entangled, which will further induce a bending of the DNA origami. The bound DOTAP molecules will also effectively screen the electrostatic repulsion between the phosphate groups in the DNA origamis, which facilitates the rather tight packing of the 6HBs.

For the multilamellar complexes formed using the 6HB, the average interlamellar spacing measured from the TEM image is 5.1 ± 0.7 nm (Figure 3b). Similar interlamellar spacings have also been determined when the two other DNA origamis were employed (see S11 and S14), which suggest that the observed condensed lamellar structures are in this case mostly alternating DOTAP bilayers separated by a counterion rich water gap. The determined interlamellar distances are also in good agreement with the previously reported interlamellar periodicities of hydrated multilayer DOTAP films (4.85 nm[43] respective 4.2–4.9 nm[44]). In solution, the thickness of a DOTAP bilayer has been determined as 3.72 ± 0.03 nm,[45] but the interlamellar distances in multilamellar assemblies will be higher than this due to the repulsion between the cationic head groups and swelling of the lamellar phase in excess water.[10] In the case of 6HB, the observed structural dimensions also match with the thickness of the DNA origami and therefore, as shown in Figure

3a, the multilamellar structure could also be alternating layers of 6HB and lipid bilayers resulting from the folding of the 6HBs into 'ball of yarn'-like structures.

In addition to conventional TEM, we also investigated the formed assemblies in their native state using cryogenic transmission electron microscopy (cryo-TEM). However, the vitrified specimens were prone to electron beam radiation damage, which set limitation to the performed analysis. Nevertheless, similar multilamellar structures as in the conventional TEM images were observed in the cryo-TEM images of the unstained, vitrified samples (Figure 3c), which confirms that the formed lamellar structures are not drying artefacts. Further, cryo-TEM investigation of DOTAP alone in aqueous ethanol solution (S4) shows merely differently sized unilamellar liposomes, which supports the hypothesis that the DNA origami function as a template for the formation of the observed multilamellar lipid complexes.

To gain additional insight into the structural morphology of the lipid assemblies, we conducted transmission electron tomography (ET) reconstruction of the formed complexes (Figure 3d, S15, S16). The reconstructed 3D electron density map of the assemblies and cross-sectional views through the structure clearly suggest that the formed complexes are made up of a dense, highly interconnected network. Interestingly, we also observed from the ET reconstruction and the TEM images (Figure 2) that the assemblies formed using the 6HB favor a more concentric lamellar structure, whereas the complexes formed using the 60HB and plate tend to have a more stacked lamellar arrangement. DOTAP has zero spontaneous curvature (lipid packing parameter, $P \sim 0$) and will therefore prefer a flat lamellar arrangement.[11,38] However, in this case, when DOTAP is electrostatically assembled with DNA origamis, the lipid packing behavior may be templated by the underlaying DNA origami, which could explain the observed difference in the lamellar arrangement. As already discussed, the 6HB are rather flexible and wrap into 'ball of yarn'-like

assemblies with high curvature when combined with DOTAP. Both the 60HB and the plate, on the other hand, are hexahedrons with low curvature and hence DOTAP tend to adopt a more stacked lamellar arrangement when these two are employed.

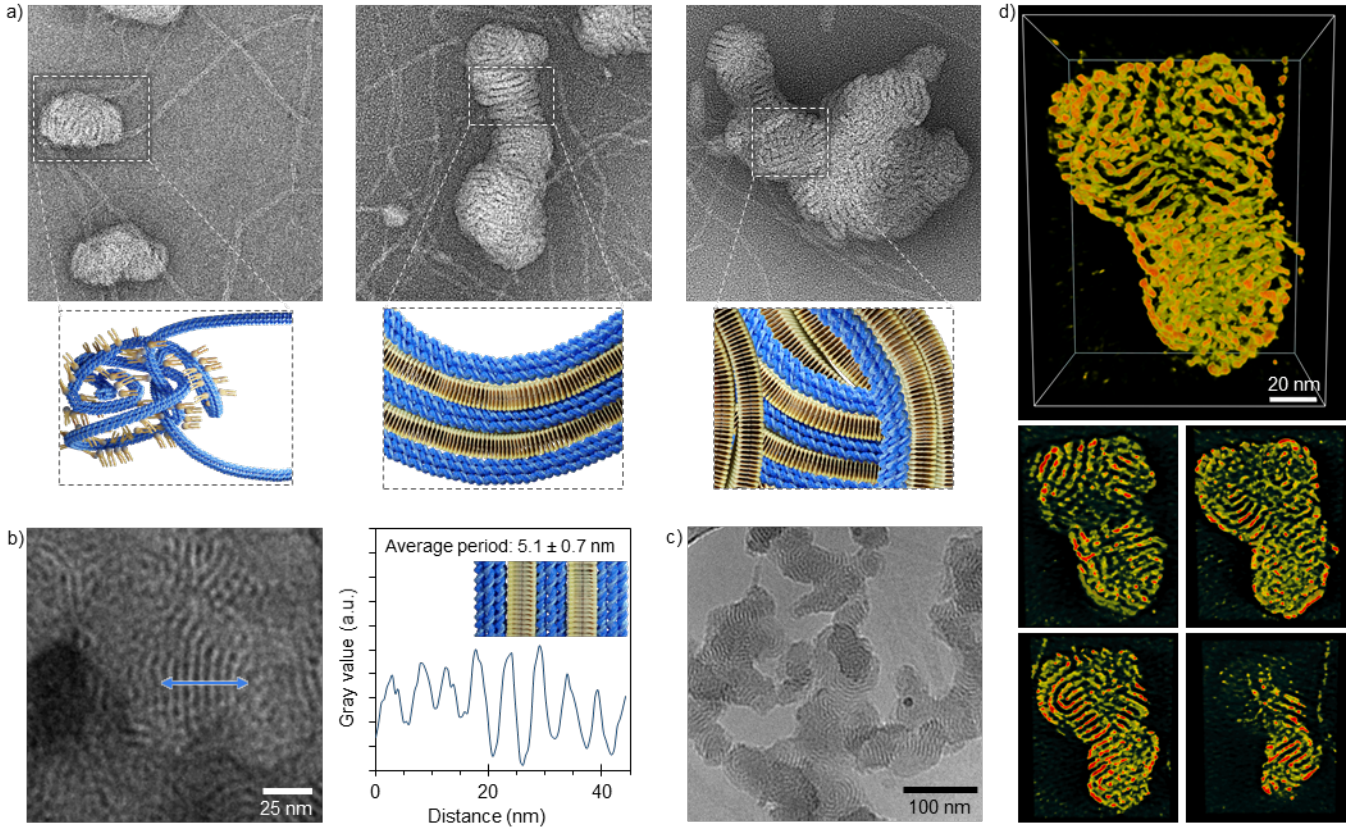

Figure 3. Structural characterization of the lipid complexes formed using the 6HB. (a) HR-TEM images (250 nm × 250 nm) of negatively stained assemblies formed at a stoichiometric ratio of n_{DOTAP}/n_{6HB} ~2500. The areas marked with dotted white lines are schematically presented below respective image. (b) A magnified view of a negatively stained complex formed at a stoichiometric ratio of n_{DOTAP}/n_{6HB} ~7500 (left) and an integrated profile along the blue line in the TEM image. (c) Cryo-TEM image of an unstained, plunge-frozen sample at a stoichiometric ratio of n_{DOTAP}/n_{6HB} ~5000. (d) Transmission electron tomography (ET) reconstruction of an assembly formed at a

stoichiometric ratio of n_{DOTAP}/n_{6HB} ~2500. The insets below the ET reconstruction show representative vertical cross-sections of the internal structure (depths of 10, 20, 28 and 36 nm)

To get information about the structural composition of the multilamellar structures and to further confirm that the DNA origamis are inside the complexes, we performed energy-dispersive X-ray spectroscopy (EDS) analysis in scanning transmission electron microscopy (STEM) mode (Figure 4a and b, S17-S19) for selected areas in the samples. DNA origamis contain, due to the phosphate groups in the DNA backbone, many phosphorous atoms and an appreciable phosphorous signal could therefore reveal the DNA origamis in the sample. Neither the carbon support film nor the DOTAP contain phosphorous and will thus not alone generate a phosphorous peak in the EDS spectra. In all studied samples, the strongest phosphorus signal was observed for areas inside the multilamellar assemblies, which suggest both that the DNA origami are inside the complexes and that the DNA origamis are tightly packed together inside the lipid matrix.

In addition to plain DNA origamis, we also used 6HB with conjugated gold nanoparticles (AuNP-6HB) for the complexation. For this experiment, the 6HB design was modified by adding three single-stranded DNA (ssDNA) attachment sites to which AuNPs functionalized with complementary ssDNA oligonucleotides could hybridize (inset in Figure 4c, see Supporting Information for the preparation steps and characterization). Due to their high contrast, the AuNPs conjugated to the 6HBs could be readily identified in the TEM images and, as expected, most of the AuNPs were found inside the lipid complexes, which further indicate that also the DNA origamis are within these complexes (Figure 4c). Furthermore, similar multilamellar assemblies as previously were observed when the AuNP-6HBs were employed, which demonstrate that our

DOTAP encapsulation strategy is suitable also for more complex DNA origami functionalized with molecular components.

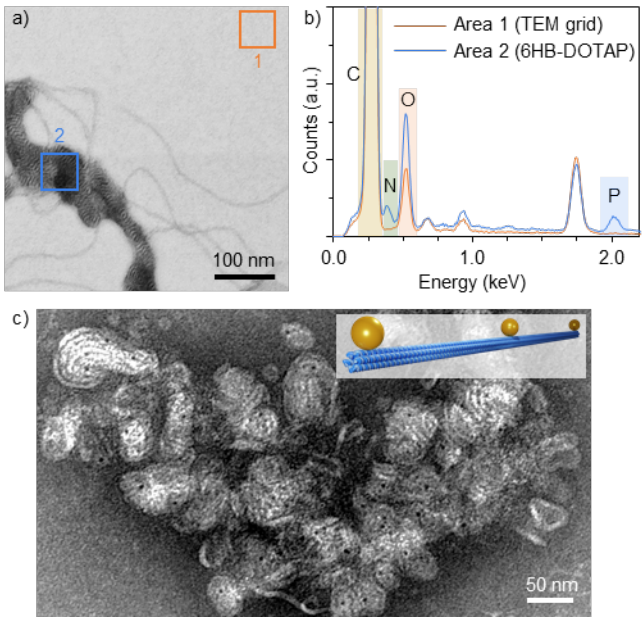

Figure 4. Verification that the DNA origamis are inside the lipid assemblies. (a) Scanning transmission electron microscope (STEM) image of unstained complexes formed at a stoichiometric ratio of n_{DOTAP}/n_{6HB} ~5000. (b) Energy-dispersive X-ray spectroscopy (EDS) spectra of the areas indicated in (a). The peaks corresponding to carbon (C), nitrogen (N), oxygen (O) and phosphorous (P) are indicated in the spectra. (c) TEM image of negatively stained complexes formed using 6HB with gold nanoparticles conjugated (AuNP-6HB). The inset shows the design of the AuNP-6HB and the position of the three AuNPs.

The DNA origamis have higher stability against nuclease digestion than double stranded DNA of similar sizes,[46] however bare DNA origamis have limited resistance against enzymatic degradation in biologically relevant media.[18,27] As previously reported, various coating strategies have proven to increase the structural stability against nucleases,[28,29,31–35] and therefore we also examined whether the DNA origamis embedded in the lipid matrix could be protected against

deoxyribonuclease I (DNase I) digestion. DNase I is the most important nuclease in blood and serum and the stability against DNase I is therefore widely used as a measure to simulate the DNA origami stability also *in vivo*.[18,47] For this experiment, both plain DNA origamis and formed DNA origami – lipid complexes were incubated with increasing amounts of DNase I for 1 h at room temperature, after which the samples were analyzed by agarose gel EMSA. To ensure that the DNA origamis were completely shielded by the DOTAP molecules, a stoichiometric ratio of $n_{DOTAP}/n_{origami}$ ~7500 was used. The DNA origami concentration was kept constant at 7.5 nM in all samples, whereas the final DNase I concentration in the samples varied between 0 Kunitz units/mL and 200 Kunitz units/mL. Remarkably, the used concentrations are more than 100-fold higher than the DNase I level in blood plasma (0.34 – 0.38 Kunitz unit/mL)[48]. Further, since intact DNA origami – lipid complexes are completely retained in the gel wells, we used linear polyanionic heparin to disassemble the complexes and recover the DNA origamis after DNase I incubation but before running the agarose gel (see the Supporting Information for the details about the decomplexation).

Plain DNA origamis were readily digested by DNase I and we observed that a DNase I concentration of 50 Kunitz U/mL was enough to completely digest all three DNA origami structures within 1 hour at room temperature (Figure 5a, top panel). A significant higher resistance against DNase I digestion was observed for all DNA origamis encapsulated in the lipid matrix. For the 60HBs and plates complexed with DOTAP, a smearing of the leading band followed by the appearance of fragments with higher electrophoretic migration speeds was observed already at 50 Kunitz U/mL, which indicates that the structures begin to degrade. By monitoring the intensity decrease of the leading band, we estimated that 48 % of 60HBs and 30 % of plates were intact after the exposure to 50 Kunitz U/mL of DNase I for 1 hour (Figure 2b). Interestingly, the 6HB

appears to be better shielded against DNase I digestion by the lipid matrix than the 60HB and the plate. Even after an incubation with 150 Kunitz U/mL of DNase I for 1 hour approximately 60 % of 6HB were still intact. Due to the high mechanical flexibility and the wrapping into 'ball of yarn'-like complexes, the 6HB might be more tightly embedded in the lipid matrix, which also improves the stability against DNase I. The resistance against DNase I digestion has been reported to be highly superstructure dependent,[47] which may account for some of the differences observed in the DNase I stability among the structures. Nevertheless, the amounts of DNase I used in the experiments is well above the concentrations in normal physiological conditions and the DOTAP encapsulation thus provides a remarkably enhanced protection against enzymatic digestion in a biologically relevant media.

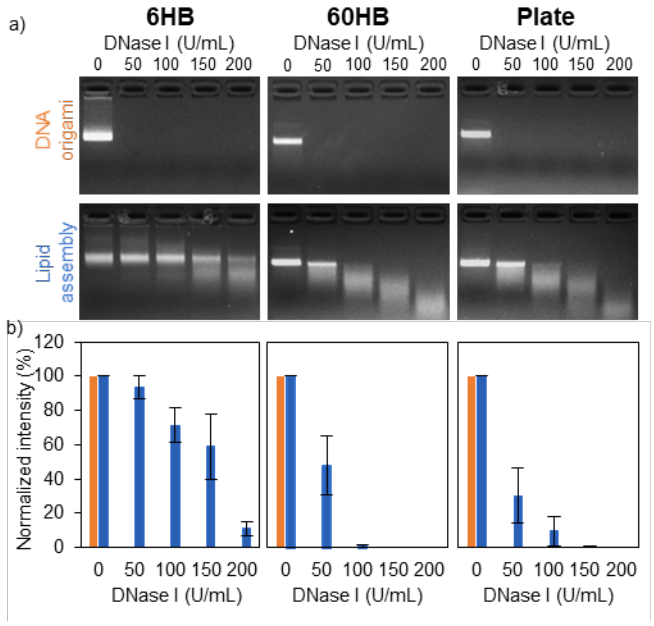

Figure 5. Protection against digestion by deoxyribonuclease I (DNase I). (a) Agarose gel electrophoresis of plain DNA origamis (top) and DNA origamis complexed with DOTAP (bottom) after incubation with increasing amounts of DNase I for 1 hour at room temperature. A stoichiometric ratio of $n_{DOTAP}/n_{origami} \sim 7500$ was used for the samples complexed with DOTAP and

these samples were disassembled with heparin before running the agarose gel. (b) Normalized agarose gel intensity for the leading band determined from three different gels. For the normalization, the gel intensity of the control sample (0 U/mL) was always marked to be 100 %. The data is given as the mean and the error bars represents standard deviations (n = 3).

CONCLUSIONS

In this work, we have demonstrated that DNA origami nanostructures can be used as template and nucleation site for the growth of multilamellar lipid assemblies. The assembly process is driven by electrostatic and hydrophobic interactions and structural characterization of the formed complexes indicates that the DNA origamis are embedded in the lipid matrix during the assembly. Furthermore, the lipid encapsulation significantly enhanced the DNA origami stability against nuclease digestion and could therefore be used as a non-toxic approach to increase the bioavailability of DNA-based nanostructures. DNA origami is a powerful tool to artificially construct and mimic cell membrane-associated structural components,[20] and therefore it is expected that hybrid materials assembled using DNA nanostructures and lipids will have applications in biology and nanomedicine in the near future.[19] However, effective strategies to assemble the hydrophobic lipids with the hydrophilic DNA origami is still needed. We have presented a straightforward and scalable method for combining these two into a hybrid nanomaterial. In addition, the method is not limited to certain DNA origami shapes, it is even compatible with DNA-based structures functionalized with molecular components, such as AuNPs. Therefore, we believe that this modular approach could find intriguing uses and provide valuable insight into the interactions between DNA origami and lipids.

ASSOCIATED CONTENT

Supporting Information. The following files are available free of charge.

Materials and full experimental methods including details on DNA origami preparation, purification and characterization, DOTAP preparation and characterization, formation of lipid assemblies and their characterization with TEM, cryo-TEM, ET-reconstruction, STEM and EDS, AuNP-6HB preparation, purification and characterization, formation of lipid complexes with AuNP-6HB and their characterization with TEM, decomplexation of lipid assemblies using heparin, EMSA to study stability against DNase I digestion. Additional data including TEM images of DNA origami, DOTAP and lipid assemblies, ET-reconstruction of lipid complexes, STEM and EDS analysis of lipid assemblies, EMSA after decomplexation with heparin, EMSA after incubation with DNase I. Design and a list of the staple strands for the DNA origami plate.

AUTHOR INFORMATION

Corresponding Author

*E-mail: veikko.linko@aalto.fi

*E-mail: mauri.kostiainen@aalto.fi

Author Contributions

The manuscript was written through contributions of all authors. All authors have given approval to the final version of the manuscript.

Notes

The authors declare no competing financial interest.

ACKNOWLEDGMENT

This work was supported by the Academy of Finland (projects 286845 and 308578), the Swedish Cultural Foundation in Finland, the Jane and Aatos Erkko Foundation, the Sigrid Jusélius Foundation, and the Emil Aaltonen Foundation. The work was carried out under the Academy of Finland Center of Excellence Programme (2014–2019). We acknowledge the provision of facilities and technical support by Aalto University Bioeconomy Facilities and OtaNano – Nanomicroscopy Center. The authors would like to thank Heini Ijäs for assistance in the design of the DNA origami plate structure.

REFERENCES

(1) Zhang, S. Fabrication of Novel Biomaterials through Molecular Self-Assembly. *Nat. Biotechnol.* **2003**, *21*, 1171–1178. https://doi.org/10.1038/nbt874.

(2) Tresset, G. The Multiple Faces of Self-Assembled Lipidic Systems. *PMC Biophys.* **2009**, *2*, 1–25. https://doi.org/10.1186/1757-5036-2-3.

(3) Kulkarni, C. V. Lipid Crystallization: From Self-Assembly to Hierarchical and Biological Ordering. *Nanoscale* **2012**, *4*, 5779–5791. https://doi.org/10.1039/c2nr31465g.

(4) Wasungu, L.; Hoekstra, D. Cationic Lipids, Lipoplexes and Intracellular Delivery of Genes. *J. Control. Release* **2006**, *116*, 255–264. https://doi.org/10.1016/j.jconrel.2006.06.024.

(5) Zhang, S.; Xu, Y.; Wang, B.; Qiao, W.; Liu, D.; Li, Z. Cationic Compounds Used in Lipoplexes and Polyplexes for Gene Delivery. *J. Control. Release* **2004**, 100, 165–180. https://doi.org/10.1016/j.jconrel.2004.08.019.

(6) Tros de Ilarduya, C.; Sun, Y.; Düzgüneş, N. Gene Delivery by Lipoplexes and Polyplexes.

Eur. J. Pharm. **2010**, *40*, 159–170. https://doi.org/10.1016/j.ejps.2010.03.019.

(7) Liu, K.; Zheng, L.; Ma, C.; Göstl, R.; Herrmann, A. DNA-Surfactant Complexes: Self-Assembly Properties and Applications. *Che*m. *Soc. Rev.* **2017**, *46*, 5147–5172. https://doi.org/10.1039/c7cs00165g.

(8) Safinya, C. R. Structures of Lipid-DNA Complexes: Supramolecular Assembly and Gene Delivery. *Curr. Opin. Struc. Biol.*, **2001**, *11*, 440–448. https://doi.org/10.1016/S0959-440X(00)00230-X.

(9) Ma, B.; Zhang, S.; Jiang, H.; Zhao, B.; Lv, H. Lipoplex Morphologies and Their Influences on Transfection Efficiency in Gene Delivery. *J. Control. Release* **2007**, *123*, 184–194. https://doi.org/10.1016/j.jconrel.2007.08.022.

(10) Rädler, J. O.; Koltover, I.; Salditt, T.; Safinya, C. R. Structure of DNA-Cationic Liposome Complexes: DNA Intercalation in Multilamellar Membranes in Distinct Interhelical Packing Regimes. *Science* **1997**, *275* , 810–814. https://doi.org/10.1126/science.275.5301.810.

(11) Koltover, I.; Salditt, T.; Rädler, J. O.; Safinya, C. R. An Inverted Hexagonal Phase of Cationic Liposome-DNA Complexes Related to DNA Release and Delivery. *Science* **1998**, *281*, 78–81. https://doi.org/10.1126/science.281.5373.78.

(12) Ewert, K. K.; Evans, H. M.; Zidovska, A.; Bouxsein, N. F.; Ahmad, A.; Safinya, C. R. A Columnar Phase of Dendritic Lipid-Based Cationic Liposome-DNA Complexes for Gene Delivery: Hexagonally Ordered Cylindrical Micelles Embedded in a DNA Honeycomb Lattice. *J. Am. Chem. Soc.* **2006**, *128*, 3998–4006. https://doi.org/10.1021/ja055907h.

(13) Leal, C.; Ewert, K. K.; Bouxsein, N. F.; Shirazi, R. S.; Li, Y.; Safinya, C. R. Stacking of Short DNA Induces the Gyroid Cubic-to-Inverted Hexagonal Phase Transition in Lipid-

DNA Complexes. *Soft Matter* **2013**, *9*, 795–804. https://doi.org/10.1039/c2sm27018h.

(14) Seeman, N. C.; Sleiman, H. F. DNA Nanotechnology. *Nat. Rev. Mater.*, 2017, **3**, 17068. https://doi.org/10.1038/natrevmats.2017.68.

(15) Hong, F.; Zhang, F.; Liu, Y.; Yan, H. DNA Origami: Scaffolds for Creating Higher Order Structures. *Chem. Rev.* **2017**, *117*, 12584–12640. https://doi.org/10.1021/acs.chemrev.6b00825.

(16) Rothemund, P. W. K. Folding DNA to Create Nanoscale Shapes and Patterns. *Nature*. **2006,** *440*, 297–302. https://doi.org/10.1038/nature04586.

(17) Li, J.; Fan, C.; Pei, H.; Shi, J.; Huang, Q. Smart Drug Delivery Nanocarriers with Self-Assembled DNA Nanostructures. *Adv. Mater.* **2013**, *25*, 4386–4396. https://doi.org/10.1002/adma.201300875.

(18) Keller, A.; Linko, V. Challenges and Perspectives of DNA Nanostructures in Biomedicine. *Angew. Chem. Int. Ed. Engl.* **2020**. https://doi.org/10.1002/anie.201916390.

(19) Langecker, M.; Arnaut, V.; List, J.; Simmel, F. C. DNA Nanostructures Interacting with Lipid Bilayer Membranes. *Acc. Chem. Res.* **2014**, *47*, 1807–1815. https://doi.org/10.1021/ar500051r.

(20) Shen, H.; Wang, Y.; Wang, J.; Li, Z.; Yuan, Q. Emerging Biomimetic Applications of DNA Nanotechnology. *ACS Appl. Mater. Interfaces* **2019**, *11*, 13859–13873. https://doi.org/10.1021/acsami.8b06175.

(21) Bae, W.; Kocabey, S.; Liedl, T. DNA Nanostructures in Vitro, in Vivo and on Membranes. *Nano Today*. **2019**, *26*, 98–107. https://doi.org/10.1016/j.nantod.2019.03.001.

(22) Maune, H. T.; Han, S. P.; Barish, R. D.; Bockrath, M.; Iii, W. A. G.; Rothemund, P. W. K.; Winfree, E. Self-Assembly of Carbon Nanotubes into Two-Dimensional Geometries

Using DNA Origami Templates. *Nat. Nanotechnol.* **2010**, *5*, 61–66. https://doi.org/10.1038/nnano.2009.311.

(23) Kuzyk, A.; Schreiber, R.; Fan, Z.; Pardatscher, G.; Roller, E. M.; Högele, A.; Simmel, F. C.; Govorov, A. O.; Liedl, T. DNA-Based Self-Assembly of Chiral Plasmonic Nanostructures with Tailored Optical Response. *Nature* **2012**, *483*, 311–314. https://doi.org/10.1038/nature10889.

(24) Julin, S.; Korpi, A.; Nonappa; Shen, B.; Liljeström, V.; Ikkala, O.; Keller, A.; Linko, V.; Kostiainen, M. A. DNA Origami Directed 3D Nanoparticle Superlattice: Via Electrostatic Assembly. *Nanoscale* **2019**, *11*, 4546–4551. https://doi.org/10.1039/c8nr09844a.

(25) Jiang, T.; Meyer, T. A.; Modlin, C.; Zuo, X.; Conticello, V. P.; Ke, Y. Structurally Ordered Nanowire Formation from Co-Assembly of DNA Origami and Collagen-Mimetic Peptides. *J. Am. Chem. Soc.* **2017**, *139*, 14025–14028. https://doi.org/10.1021/jacs.7b08087.

(26) Ramakrishnan, S.; Ijäs, H.; Linko, V.; Keller, A. Structural Stability of DNA Origami Nanostructures under Application-Specific Conditions. *Comp. Struct. Biotech. J.* **2018**, *16*, 342–349. https://doi.org/10.1016/j.csbj.2018.09.002.

(27) Bila, H.; Kurisinkal, E. E.; Bastings, M. M. C. Engineering a Stable Future for DNA-Origami as a Biomaterial. *Biomater. Sci.* **2019**, *7*, 532–541. https://doi.org/10.1039/c8bm01249k.

(28) Perrault, S. D.; Shih, W. M. Virus-Inspired Membrane Encapsulation of DNA Nanostructures to Achieve in Vivo Stability. *ACS Nano* **2014**, *8*, 5132–5140. https://doi.org/10.1021/nn5011914.

(29) Anastassacos, F. M.; Zhao, Z.; Zeng, Y.; Shih, W. M. Glutaraldehyde Cross-Linking of

Oligolysines Coating DNA Origami Greatly Reduces Susceptibility to Nuclease Degradation. *J. Am. Chem. Soc.* **2020**, *142*, 3311–3315. https://doi.org/10.1021/jacs.9b11698.

(30) Kiviaho, J. K.; Linko, V.; Ora, A.; Tiainen, T.; Järvihaavisto, E.; Mikkilä, J.; Tenhu, H.; Nonappa; Kostiainen, M. A. Cationic Polymers for DNA Origami Coating-Examining Their Binding Efficiency and Tuning the Enzymatic Reaction Rates. *Nanoscale* **2016**, *8*, 11674–11680. https://doi.org/10.1039/c5nr08355a.

(31) Agarwal, N. P.; Matthies, M.; Gür, F. N.; Osada, K.; Schmidt, T. L. Block Copolymer Micellization as a Protection Strategy for DNA Origami. *Angew. Chemie - Int. Ed.* **2017**, *56*, 5460–5464. https://doi.org/10.1002/anie.201608873.

(32) Ponnuswamy, N.; Bastings, M. M. C.; Nathwani, B.; Ryu, J. H.; Chou, L. Y. T.; Vinther, M.; Li, W. A.; Anastassacos, F. M.; Mooney, D. J.; Shih, W. M. Oligolysine-Based Coating Protects DNA Nanostructures from Low-Salt Denaturation and Nuclease Degradation. *Nat. Commun.* **2017**, *8*. https://doi.org/10.1038/ncomms15654.

(33) Ahmadi, Y.; De Llano, E.; Barišić, I. (Poly)Cation-Induced Protection of Conventional and Wireframe DNA Origami Nanostructures. *Nanoscale* **2018**, *10*, 7494–7504. https://doi.org/10.1039/c7nr09461b.

(34) Auvinen, H.; Zhang, H.; Nonappa; Kopilow, A.; Niemelä, E. H.; Nummelin, S.; Correia, A.; Santos, H. A.; Linko, V.; Kostiainen, M. A. Protein Coating of DNA Nanostructures for Enhanced Stability and Immunocompatibility. *Adv. Healthc. Mater.* **2017**, *6*, 1700692. https://doi.org/10.1002/adhm.201700692.

(35) Xu, X.; Fang, S.; Zhuang, Y.; Wu, S.; Pan, Q.; Li, L.; Wang, X.; Sun, X.; Liu, B.; Wu, Y. Cationic Albumin Encapsulated DNA Origami for Enhanced Cellular Transfection and

Stability. *Materials* **2019**, *16*, 949. https://doi.org/10.3390/ma12060949.

(36) Mikkilä, J.; Eskelinen, A. P.; Niemelä, E. H.; Linko, V.; Frilander, M. J.; Törmä, P.; Kostiainen, M. A. Virus-Encapsulated DNA Origami Nanostructures for Cellular Delivery. *Nano Lett.* **2014**, *14*, 2196–2200. https://doi.org/10.1021/nl500677j.

(37) Kielar, C.; Xin, Y.; Shen, B.; Kostiainen, M. A.; Grundmeier, G.; Linko, V.; Keller, A. On the Stability of DNA Origami Nanostructures in Low-Magnesium Buffers. *Angew. Chemie - Int. Ed.* **2018**, *57*, 9470–9474. https://doi.org/10.1002/anie.201802890.

(38) Meisel, J. W.; Gokel, G. W. A Simplified Direct Lipid Mixing Lipoplex Preparation: Comparison of Liposomal-, Dimethylsulfoxide-, and Ethanol-Based Methods. *Sci. Rep.* **2016**, *6*, 1–12. https://doi.org/10.1038/srep27662.

(39) Kostiainen, M. A.; Hiekkataipale, P.; Laiho, A.; Lemieux, V.; Seitsonen, J.; Ruokolainen, J.; Ceci, P. Electrostatic Assembly of Binary Nanoparticle Superlattices Using Protein Cages. *Nat. Nanotechnol.* **2013**, *8*, 52–56. https://doi.org/10.1038/nnano.2012.220.

(40) Douglas, S. M.; Marblestone, A. H.; Teerapittayanon, S.; Vazquez, A.; Church, G. M.; Shih, W. M. Rapid Prototyping of 3D DNA-Origami Shapes with CaDNAno. *Nucleic Acids Res.* **2009**, *37*, 5001–5006. https://doi.org/10.1093/nar/gkp436.

(41) Battaglia, G.; Tomas, S.; Ryan, A. J. Lamellarsomes: Metastable Polymeric Multilamellar Aggregates. *Soft Matter* **2007**, *3*, 470–475. https://doi.org/10.1039/b605493e.

(42) Matulis, D.; Rouzina, I.; Bloomfield, V. A. Thermodynamics of Cationic Lipid Binding to DNA and DNA Condensation: Roles of Electrostatics and Hydrophobicity. *J. Am. Chem. Soc.* **2002**, *124*, 7331–7342. https://doi.org/10.1021/ja0124055.

(43) Caminiti, R.; Caracciolo, G.; Pisani, M.; Bruni, P. Effect of Hydration on the Long-Range Order of Lipid Multilayers Investigated by in Situ Time-Resolved Energy Dispersive X-

Ray Diffraction. *Chem. Phys. Lett.* **2005**, *409*, 331–336. https://doi.org/10.1016/j.cplett.2005.05.044.

(44) Cavalcanti, L. P.; Konovalov, O.; Haas, H. X-Ray Diffraction from Paclitaxel-Loaded Zwitterionic and Cationic Model Membranes. *Chem. Phys. Lipids* **2007**, *150*, 58–65. https://doi.org/10.1016/j.chemphyslip.2007.06.219.

(45) Rädler, J. O.; Koltover, I.; Jamieson, A.; Salditt, T.; Safinya, C. R. Structure and Interfacial Aspects of Self-Assembled Cationic Lipid-DNA Gene Carrier Complexes. *Langmuir* **1998**, *14*, 4272–4283. https://doi.org/10.1021/la980360o.

(46) Castro, C. E.; Kilchherr, F.; Kim, D. N.; Shiao, E. L.; Wauer, T.; Wortmann, P.; Bathe, M.; Dietz, H. A Primer to Scaffolded DNA Origami. *Nat. Methods* **2011**, *8*, 221–229. https://doi.org/10.1038/nmeth.1570.

(47) Ramakrishnan, S.; Shen, B.; Kostiainen, M. A.; Grundmeier, G.; Keller, A.; Linko, V. Real-Time Observation of Superstructure-Dependent DNA Origami Digestion by DNase I Using High-Speed Atomic Force Microscopy. *ChemBioChem* **2019**, *20*, 2818–2823. https://doi.org/10.1002/cbic.201900369.

(48) Cherepanova, A.; Tamkovich, S.; Pyshnyi, D.; Kharkova, M.; Vlassov, V.; Laktionov, P. Immunochemical Assay for Deoxyribonuclease Activity in Body Fluids. *J. Immunol. Methods* **2007**, *325*, 96–103. https://doi.org/10.1016/j.jim.2007.06.004.